

Searching for Planets in the Hyades V: Limits on Planet Detection in the Presence of Stellar Activity ¹

Diane B. Paulson²

Department of Astronomy, University of Texas, Austin, TX 78712

apodis@umich.edu

William D. Cochran

McDonald Observatory, University of Texas, Austin, TX 78712

wdc@astro.as.utexas.edu

and

Artie P. Hatzes

Thüringer Landessternwarte Tautenburg, D-07778 Tautenburg, Germany

ABSTRACT

We present the results of a radial velocity survey of a sample of Hyades stars, and discuss the effects of stellar activity on radial velocity measurements. The level of radial velocity scatter due to rotational modulation of stellar surface features for the Hyades is in agreement with the predictions of Saar & Donahue (1997)- the maximum radial velocity rms of up to $\sim 50 \text{ m s}^{-1}$, with an average rms of $\sim 16 \text{ m s}^{-1}$. In this sample of 94 stars, we find 1 new binary, 2 stars with linear trends indicative of binary companions, and no close-in giant planets. We discuss the limits on extrasolar planet detection in the Hyades and the constraints imposed on radial velocity surveys of young stars.

Subject headings: clusters: open (Hyades) — stars: planetary systems — techniques: radial velocities — stars: activity

²Current Address: Department of Astronomy, University of Michigan, Ann Arbor, MI 48109

¹Data presented herein were obtained at the W.M. Keck Observatory, which is operated as a scientific partnership among the California Institute of Technology, the University of California and the National Aeronautics and Space Administration. The Observatory was made possible by the generous financial support of the W.M. Keck Foundation. Additional data were obtained with the Hobby-Eberly Telescope which is operated by McDonald Observatory on behalf of the University of Texas at Austin, the Pennsylvania State University, Stanford University, Ludwig-Maximilians- Universität München, and Georg-August-Universität Göttingen.

1. Introduction

Radial velocity (v_r) surveys for extrasolar planets have been extremely successful (e.g. Butler et al. 1996). These surveys have, however, largely excluded young, active stars (Vogt et al. 2002; Cumming et al. 1999; Saar & Donahue 1997). The reason given was that the activity levels of young stars is significant enough to cause large variations in the measured v_r . Although it does not introduce a true v_r shift (e.g. Saar & Donahue 1997, hereafter SD97, Hatzes 2002), the apparent shift is caused by a change in the line shape of the absorption features. SD97 quantify the predicted amplitude of this phenomenon, and it has been observationally confirmed by several groups (e.g. Queloz et al. 2001; Henry et al. 2002; Paulson et al. 2004; Saar & Fischer 2000; Saar et al. 1998). While detection of extrasolar planets around young stars will be complicated by these spectral line profile variations, there is much to learn about the frequency of planets and their orbital characteristics at all stellar ages. So, it is necessary to learn the limitations of the techniques employed in planet detection and then proceed (if possible) with planet searches.

We present here the results of the radial velocity search for extrasolar planets in a sample of Hyades dwarfs. Primarily, we discuss the mean level of radial velocity noise caused by stellar magnetic activity and the possibilities of detecting planets in Hyades-aged stars.

2. Observations and Analysis

We have been studying a sample of Hyades dwarfs ranging from spectral classes F5 to M2 with the Keck I High Resolution Echelle Spectrometer (Vogt et al. 1994). The observations and analysis of the v_r data are discussed in Cochran et al. (2002). While we made every attempt to include only stars which were not binaries, we discovered some stars which have too high v_r rms to be non-binaries. These stars are discussed in §5.2.

The measurement of v_r involves using an I_2 gas absorption cell as a standard velocity reference (Valenti et al. 1995). A signal-to-noise ratio (S/N) of ~ 150 -300 is achieved at 5000\AA with resolution $R \simeq 60,000$. In the case of high S/N (≥ 200), we achieve an internal precision ~ 3 -4 m s^{-1} for a given star (Cochran et al. 2002); while a spectrum with S/N ~ 100 yields precision of $\sim 6 \text{ m s}^{-1}$. In addition, the exposure times are maintained at ≤ 15 minutes. We use standard IRAF packages to reduce the CCD images and extract the observed spectra. The v_r measurements are made using a program called RADIAL (developed at the University of Texas, UT, and McDonald Observatory) to measure precise radial velocities. This program was adapted for use with data from all of the planet search programs affiliated with UT. Discussions of RADIAL may be found in Cochran et al. (1997) and Hatzes et al. (2000). The v_r measurements of all data in this sample obtained with the Keck telescope are listed in Table 1. Measurements of vB 15, vB 18 and vB 153 taken with the HRS at the Hobby-Eberly Telescope (HET) are discussed and listed in Paulson et al. (2004) (hereafter PSC04).

3. Results

While the target sample was selected in part on non-binarity, a handful of binaries did end up in our sample. The stars listed in Table 2 show either significant linear trends (most likely binaries) or a defined binary orbit (vB 88). The measured v_r of binary stars and stars with significant linear trends are shown in Figure 1. Three binaries discovered by Patience et al. (1998) were not removed from the sample in the initial compilation of targets. These are noted in the Column 3 of Table 2. Stars which only have a small slope (i.e. those with $\sigma_{v_r} \sim 40 \text{ m s}^{-1}$) have not been included in this table. vB 88 appears to have almost completed 1 orbit. A *tentative* solution (shown in Figure 1) gives an $m \sin i = 0.07 M_\odot$. Using the measured $v \sin i$ for vB 88 and an estimate of the true rotational velocity as derived by Paulson et al. (2003), we estimate the mass of the companion to be $\sim 0.86 \pm 0.31 M_\odot$, most likely a K dwarf, to the F8V parent star. While $0.31 M_\odot$ is the formal error, we note that if the mass were much larger than $0.86 M_\odot$, we would see a double lined spectrum and we see no indication of this in the vB 88 spectra. So, $0.86 M_\odot$ is most likely an upper limit to the true mass. The orbital parameters for this binary companion are listed in Table 3.

With three exceptions discussed later in this section (those showing significant long-period trends) and 1 star with poor sampling but with velocity rms of 72 m s^{-1} , the remaining stars show no significant linear trends (with rms (σ_{v_r}) $\leq 40 \text{ m s}^{-1}$). Table 4 lists the program stars, the rms of the observations with internal errors removed ($\sigma_{v_r, \text{int}}$) and the average internal error of the observations for each star (σ_{int}). This is a summary of the observations presented in Table 1. Figure 2 shows a histogram of the σ_{v_r} for the program stars excluding binaries and stars with linear trends. The internal v_r errors have been removed. We note that the majority of stars have $\sim 5 \leq \sigma_{v_r} \leq 25 \text{ m s}^{-1}$, which is what we expect from stars of this activity level and age (SD97, PSC04). In PSC04, we showed that some stars in the sample display v_r variations of $\sim 40 \text{ m s}^{-1}$ due to stellar active regions. Therefore, the stars with $\sigma_{v_r} \sim 50 \text{ m s}^{-1}$ could also suffer from severe effects of activity. It is of interest that we do not find any stars in this sample with very large σ_{v_r} ($\geq 100 \text{ m s}^{-1}$) with suggestive short periods, thus no “hot Jupiters” with mass $\geq 1 M_{Jup}$.

To explore the spread in σ_{v_r} in the sample, we compared the σ_{v_r} of each star with the measured rotational velocity ($v \sin i$) from Paulson et al. (2003). Although a little less than half of the program stars have measured $v \sin i$, we are still able to see an obvious trend in the data (see Figure 3- σ_{v_r} versus $v \sin i$, with binaries and stars with linear trends excluded and internal v_r errors removed). While there is significant scatter in the figure, a trend is still present. The location of active regions, the fraction of the surface covered by activity, the rotational velocity and the inclination of the stars all play significant roles in the measured v_r . The higher the $v \sin i$, the more broadened the spectral absorption features will be. The internal error becomes larger with increased $v \sin i$ (see Figure 4), as determination of the line center becomes increasingly difficult. As the inclination of the star decreases (becomes pole-on) lower σ_{v_r} is expected. This is because the most significant effect of active regions in this age of star (e.g. SD97) is short-period variations due to the rotational modulation of the features across the stellar surface. Take a simple case which assumes active regions are equatorial. When the star is pole-on (0°), variations of this nature will diminish and

similarly, when the star is face-on (90°), the effect will be at a maximum. Certainly, the larger fraction of the stellar surface covered by active regions will cause larger amplitude variations and the physical location of the features will cause variable effects on the line shape (and thus, the measured v_r). It is not surprising, then, that there are a few stars with very large σ_{v_r} , as statistically, a few stars should have very low inclinations. This effect of increased σ_{v_r} with increased $v \sin i$ is also predicted by A. Hatzes (2003, private communication) and discussed in SD97. Additionally, scatter in σ_{v_r} (in Figure 3) at a given $v \sin i$ is caused by star-to-star variations in the overall activity level. Although the stars do not show cyclic behavior in chromospheric activity, the overall level of activity varies.

As also shown in PSC04, some Hyades stars (vB 153, in particular) may show long lived active regions or active longitudes. Therefore, should we detect significant periods compatible with an expected or observed rotation rate, we could explore the nature of stars which display this type of activity. Therefore, to the remaining stars, we employed the same period-finding algorithm as used in PSC04 (that of Horne & Baliunas 1986). From this technique we are able to determine the most significant periods in a data set and the false alarm probabilities (FAP) associated with each period. We also perform a bootstrap algorithm (e.g. Kürster et al. 1997) to determine a false alarm probability based solely on the data. The bootstrap method does not assume a gaussian noise distribution as do the more traditional FAPs (such as Horne & Baliunas 1986). This method randomizes the data- keeping the observed times (in JD) the same but randomly assigning the v_r observed to those JDs. The resultant “fake” data are run through the periodogram to determine the most significant period of this data. This randomization process is iterated 1000 times and a false alarm probability is the ratio of the number of times the power of the detected period in the fake data was equal to or larger than the power of the signal in the original data. If the data are pure noise, then the false alarm probability should be very high (~ 1.0). The results of this analysis are listed in Table 5 for stars which had FAPs of less than 10% in each of the two methods (Horne & Baliunas and bootstrap). We explore the actual significance of these periods in § 4.

It is not surprising that the periods we derive here are not consistent with the published values of rotation periods (P_{rot}) because active regions evolve. Table 6 lists the periods we derive versus those from literature (references included in the table notes) and predicted values from Duncan et al. (1984), where possible. Additionally, the periods derived from the Keck data for the stars which we have derived P_{rot} (from Paulson et al. 2004 for vB 15, vB 18 and vB 153) are inconsistent with each other (also see Table 6). Thus, significant phase variations have occurred in the span of observations of the data taken from Keck. Because we do not have sufficient temporal coverage, we are unable to perform detailed studies of the evolution of these active regions- the decay time or migration of the active regions.

4. Limits on Substellar Companions

Using the methods outlined in Nelson & Angel (1998, hereafter NA98) we compute analytical limits on the detectability of substellar mass companions based on the duration and accuracy of the data for each star. We then compare this to a periodogram-based analytical derivation to find significant peaks representing the significant signals in the data. At frequencies where peaks cross the analytical limits, the detection of periodic signals (either companions or periodic activity) is present at the 99% confidence level.

From Eq. 4 of NA98, the companion mass is $M_C \sin i = K(PM_\star^2(2\pi G)^{-1})^{1/3}$, where i is the inclination of the companion, P is the period sampled, K is the velocity amplitude, M_\star is the mass of the parent star, and G is the gravitational constant. We derive K and P from the above periodogram analysis and M_\star is estimated from B-V measurements (Allende Prieto & Lambert 1999) and Gray (1992). We will refer to the resultant $M_C \sin i$ as the “companion mass power spectrum” (solid curve in Figure 5).

To define the limits on companion masses detected (or significant periodicity from intrinsic sources), we must calculate the limit on the detectable velocity. K_X (Eq. 15 in NA98) is the velocity amplitude exceeded by any of the N fits to randomized data in a given period range with probability $1-X$, where X is the product of probabilities of each fit at each period sampled ($X = \mathcal{P}^n$) and n is the number of sampled periods. Thus, $K_X = 2\sigma(n^{-1} \ln(2\pi P_0(f_1 - f_2)(1 - X)^{-1}))^{1/2}$, where P_0 is the duration of the original data ($JD_{\text{final}} - JD_{\text{begin}}$) and f_1 and f_2 are the lower and upper limits, respectively, of the period intervals (in our case, 4 bins per dex). X is determined from the bootstrap “false alarm probability” described in § 3. Using K_X now in place of K in Eq. 4 (NA98), we obtain the 99% confidence level of the mass limits of companions. Shown in Figure 5 are representative cases of these calculations. We show both the Keck and HET data with two different error assumptions, described below, for 3 stars. The Keck data for all stars show the same behavior as the three stars shown in Figure 5. Thus, we only show here these three because we also have data from the HET for each. The histogram plot limits have been suppressed at 1 year and 11 years for HET and Keck data, respectively.

The dashed histogram lines in Figure 5 assume that the only error in the observations are internal effects ($\sim 4\text{-}7 \text{ m s}^{-1}$). In the HET data (left column), we discover significant peaks crossing the 99% threshold. This tells us that there are significant periods at these crossings. However, these significant periods do not correspond to companions but to the rotational period of the star and aliases thereof. For the Keck data (right column), there are several crossings. This is expected as the sampling is extremely poor. There are $\sim 15\text{-}20$ observations of these stars over the course of 6 years, and many “significant” periods can be derived with this quality of sampling.

A far superior assumption, and that recommended by NA98, is that the error in the observations is not only due to internal errors but also due to the rotational modulation of active regions. For this, we assume an error equal to the mean v_r rms for the sample ($\sim 16 \text{ m s}^{-1}$, ignoring stars with linear trends and binary stars). Thus, any period spikes that cross the 99% threshold *should*

come from external sources (stellar and substellar companions). The calculation using this assumption is depicted by the solid histogram lines in Figure 5. We note that for all non-binary stars, there are absolutely no companion mass power spectrum crossings of the 99% threshold for stars in these Keck data. The binary stars have insufficient phase coverage. So, the threshold crossings are beyond the reasonable limits of the calculations described above.

Thus, we can use this method for determining the value of “significant” periods derived from a periodogram analysis quite apart from a calculated false alarm probability.

In general, we can provide constraints on the characteristics of systems which are detectable around young stars via the radial velocity technique, also employing the methods in NA98. Figure 6 presents an analysis for stars of Hyades age with different sampling. Both panels show the K velocity semi-amplitude versus orbital period. The histograms are the limits for a 99% confidence detection. The solid histogram (a) represents sampling similar to that which we observed from Keck, while the dotted histogram (b) is similar to the sampling we obtained from HET. The dotted histogram has been suppressed beyond 1 year. The two curves shown are for reference- the solid curve (c) is a $1 M_{Jup}$ companion and the dotted curve (d) is a $3 M_{Jup}$ companion. These curves are the K velocities of companions given that they are in orbits with zero eccentricity and are companions to a $1 M_{\odot}$ star with 90° inclination. The velocity-period space laying above the histograms are detectable with 99% confidence. So, for example, the top panel representing data with errors (radial velocity jitter from activity + internal errors) of $\sigma=16 \text{ m s}^{-1}$ shows that a $1 M_{Jup}$ companion is only detectable if it has periods less than ~ 100 days with only a few observations a year for 5 years and is detectable if with longer orbital periods only if the sampling is quite good (several observations a month). On the other hand, the bottom panel shows a more realistic case, as the true noise from activity will be higher than 16 m s^{-1} if the system is edge on (corresponding to the K curves c and d which are for edge on orbits). For data with errors of $\sigma=40 \text{ m s}^{-1}$, the detectability of planets with $\lesssim 1 M_{Jup}$ becomes impossible for poor sampling. For young stars with such high levels of activity related radial velocity noise, it is only feasible to look for either very high mass companions or the data must be taken with extremely good sampling (several observations a month for ~ 3 months).

5. Discussion

We can determine significant period in data by various techniques, including those discussed in this paper. But, it is most useful to understand when significant periods are real or simply artifacts of sampling. The analysis of the periodogram produces periods with FAPs $\sim 10\%$ for several stars. Phasing the data to these periods produces periodic curves (by-eye inspection). This is inadequate. Therefore, we have employed the method of Nelson & Angel (1998) to explore the significance of detections. All short-periods detected turn out to be artifacts of the sampling and of the quality of the data.

The detection of planets around young stars is complicated by the rotational modulation of stellar active regions. The activity not only causes high levels of v_r noise but can also yield periodic variations in the measured v_r causing false detections. The procedure we adopted (Nelson & Angel 1998) picks out all significant signals given the quantity and quality of data, so we must be careful in the identification of the source of variability. In our data, we find no evidence for short-period massive planets or brown dwarfs. Finally, of the 94 stars in this sample, 6 are either suspected or identified binaries and 1 has a velocity rms which is somewhat large but further observations are required to say anything more concrete- it is still within possible “jitter” from high activity levels.

Future detection of extrasolar planets around young stars via the radial velocity method will be limited to high-mass planets and in particular, those with short orbital periods. Constraints on telescope time needed for these surveys becomes clear. In order to increase the odds of planet detection, as current planet searches have determined that only $\sim 1\%$ of stars do have “hot Jupiters”, data must be sampled several times a month which requires a great deal of allocated telescope time.

This research was partially supported by a grant from NASA administered by the American Astronomical Society. DBP and WDC are also supported by NASA grant NAG5-9227 and NSF grant AST-9808980. We would like to thank the anonymous referee for very useful suggestions in preparing this manuscript for publication.

REFERENCES

- Allende Prieto, C. & Lambert, D. L. 1999, *A&A*, 352, 555
- Butler, R. P., Marcy, G. W., Williams, E., McCarthy, C., Dosanjuh, P., & Vogt, S. S. 1996, *PASP*, 108, 500
- Cochran, W. D., Hatzes, A. P., Butler, R. P., & Marcy, G. W. 1997, *ApJ*, 483, 457
- Cochran, W. D., Hatzes, A. P., & Paulson, D. B. 2002, *AJ*, 124, 565
- Cumming, A., Marcy, G. W., & Butler, R. P. 1999, *ApJ*, 526, 890
- Duncan, D. K., Frazer, J., Lanning, H. H., Baliunas, S. L., Noyes, R. W., & Vaughan, A. H. 1984, *PASP*, 96, 707
- Gray, D. F. 1992, *The Observation and Analysis of Stellar Photospheres* (Cambridge: Cambridge University Press)
- Hatzes, A. P. 2002, *Astronomische Nachrichten*, 323, 392
- Hatzes, A. P., Cochran, W. D., McArthur, B., Baliunas, S. L., Walker, G. A. H., Campbell, B., Irwin, A. W., Yang, S., Kürster, M., Endl, M., Els, S., Butler, R. P., & Marcy, G. W. 2000, *ApJ*, 544, L145

- Henry, G. W., Donahue, R. A., & Baliunas, S. L. 2002, *ApJ*, 577
- Horne, J. H. & Baliunas, S. L. 1986, *ApJ*, 302, 757
- Kürster, M., Schmitt, J. H. M. M., Cutispoto, G., & Dennerl, K. 1997, *A&A*, 320, 831
- Lockwood, G. W., Thompson, D. T., Radick, R. R., Osborn, W. H., Baggett, W. E., Duncan, D. K., & Hartmann, L. W. 1984, *PASP*, 96, 714
- Nelson, A. F. & Angel, J. R. P. 1998, *ApJ*, 500, 940
- Patience, J., Ghez, A. M., Reid, I. N., Weinberger, A. J., & Matthews, K. 1998, *AJ*, 115, 1972
- Paulson, D. B., Saar, S. H., & Cochran, W. D. 2004, *AJ*, in press
- Paulson, D. B., Saar, S. H., Cochran, W. D., & Hatzes, A. P. 2002, *AJ*, 124, 572
- Paulson, D. B., Sneden, C., & Cochran, W. D. 2003, *AJ*, 125, 318
- Queloz, D., Henry, G. W., Sivan, J. P., Baliunas, S. L., Beuzit, J. L., Donahue, R. A., Mayor, M., Naef, D., Perrier, C., & Udry, S. 2001, *A&A*, 379, 279
- Radick, R. R., Lockwood, G. W., Skiff, B. A., & Thompson, D. T. 1995, *ApJ*, 452, 332
- Radick, R. R., Thompson, D. T., Lockwood, G. W., Duncan, D. K., & Baggett, W. E. 1987, *ApJ*, 321, 459
- Saar, S. H., Butler, R. P., & Marcy, G. W. 1998, *ApJ*, 498, L153
- Saar, S. H. & Donahue, R. A. 1997, *ApJ*, 485, 319
- Saar, S. H. & Fischer, D. 2000, *ApJ*, 534, L105
- Valenti, J. A., Butler, R. P., & Marcy, G. W. 1995, *PASP*, 107, 966
- Vogt, S. S., Allen, S. L., Bigelow, B. C., Bresee, L., Brown, B., Cantrall, T., Conrad, A., Couture, M., Delaney, C., Epps, H. W., Hilyard, D., Hilyard, D. F., Horn, E., Jern, N., Kanto, D., Keane, M. J., Kibrick, R. I., Lewis, J. W., Osborne, J., Pardeilhan, G. H., Pfister, T., Ricketts, T., Robinson, L. B., Stover, R. J., Tucker, D., Ward, J., & Wei, M. Z. 1994, *Proc. Soc. Photo-opt. Inst. Eng.*, 2198, 362
- Vogt, S. S., Butler, R. P., Marcy, G. W., Fischer, D. A., Pourbaix, D., Apps, K., & Laughlin, G. 2002, *ApJ*, 568, 352

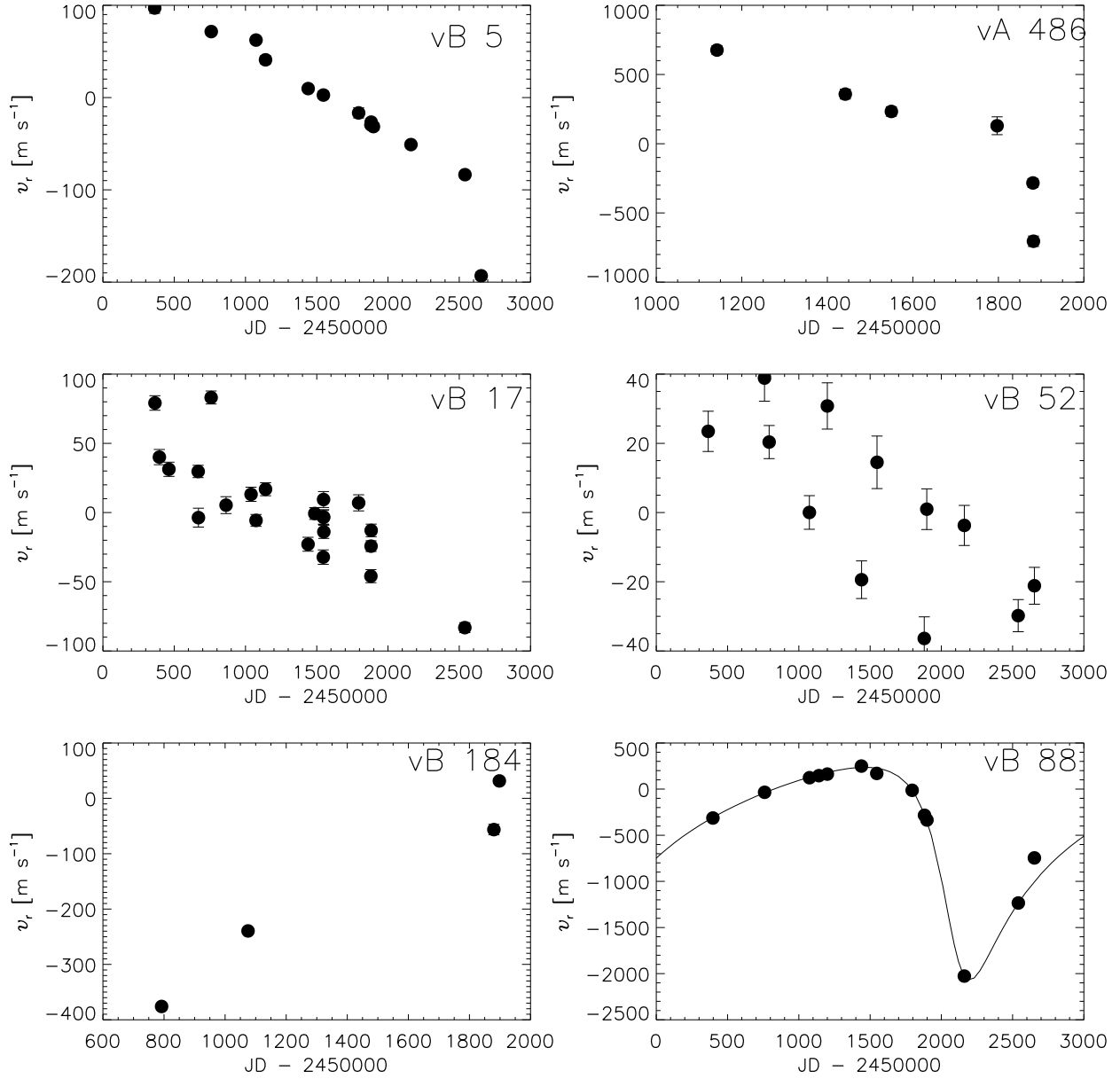


Fig. 1.— Known binaries and stars with linear trends (suspected binaries). The orbital fit to the v_r data for vB 88 is shown along with its v_r data. Internal error bars are shown.

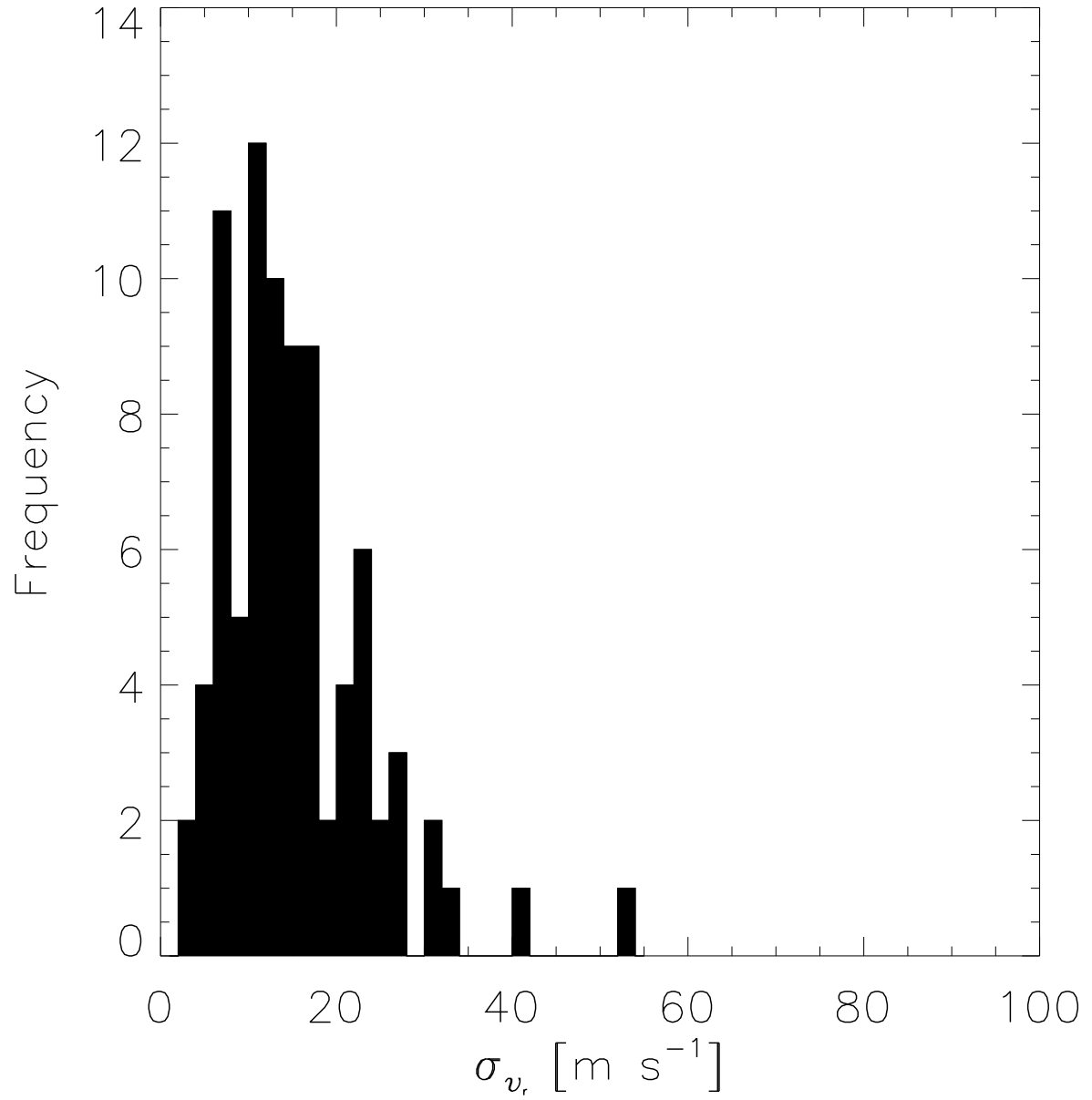


Fig. 2.— Histogram of the rms scatter in the program stars, excluding binary stars and stars with linear trends.

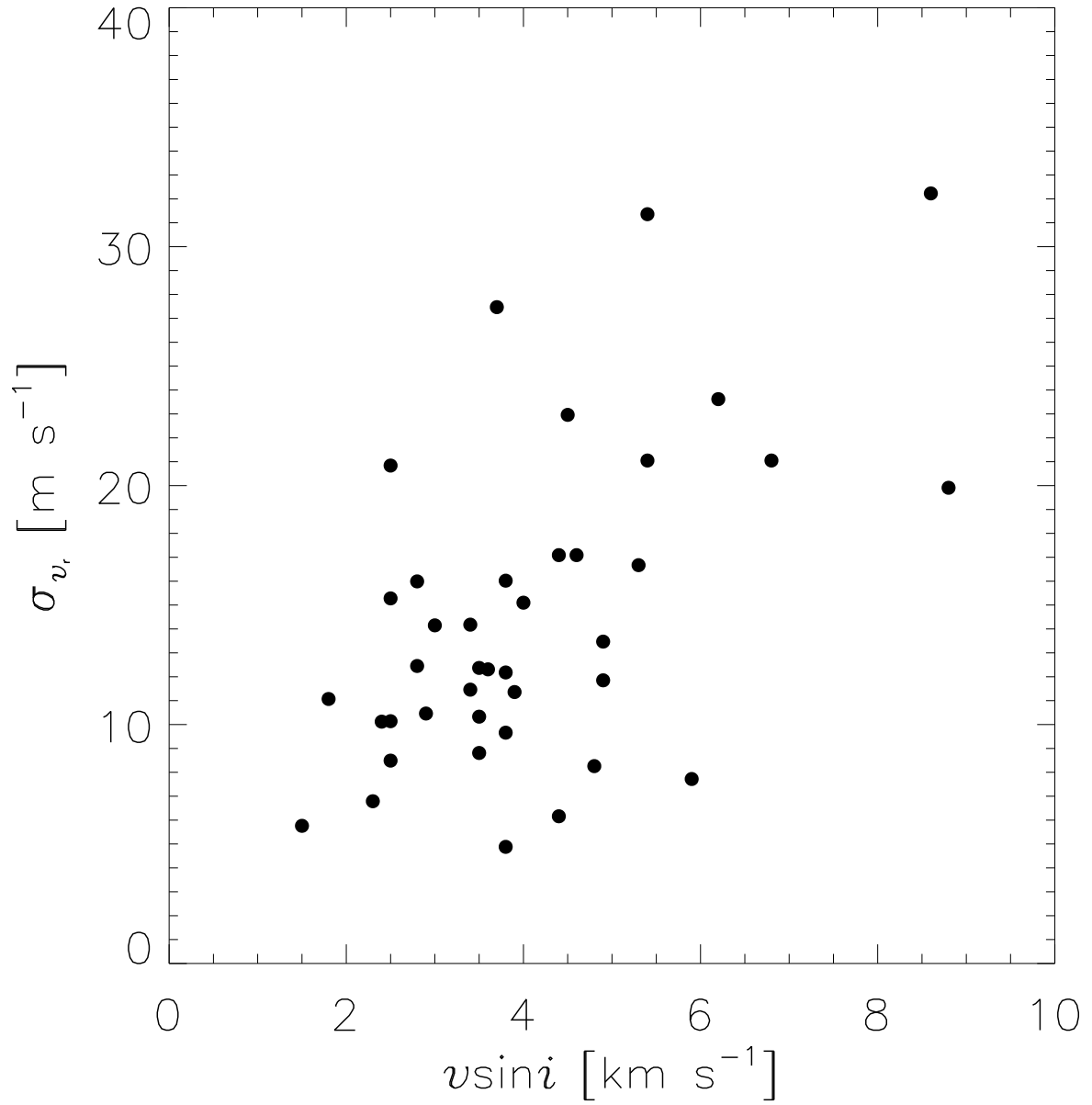


Fig. 3.— The rms scatter in the program stars versus the measured $v \sin i$. Stars with linear trends and binaries have not been included.

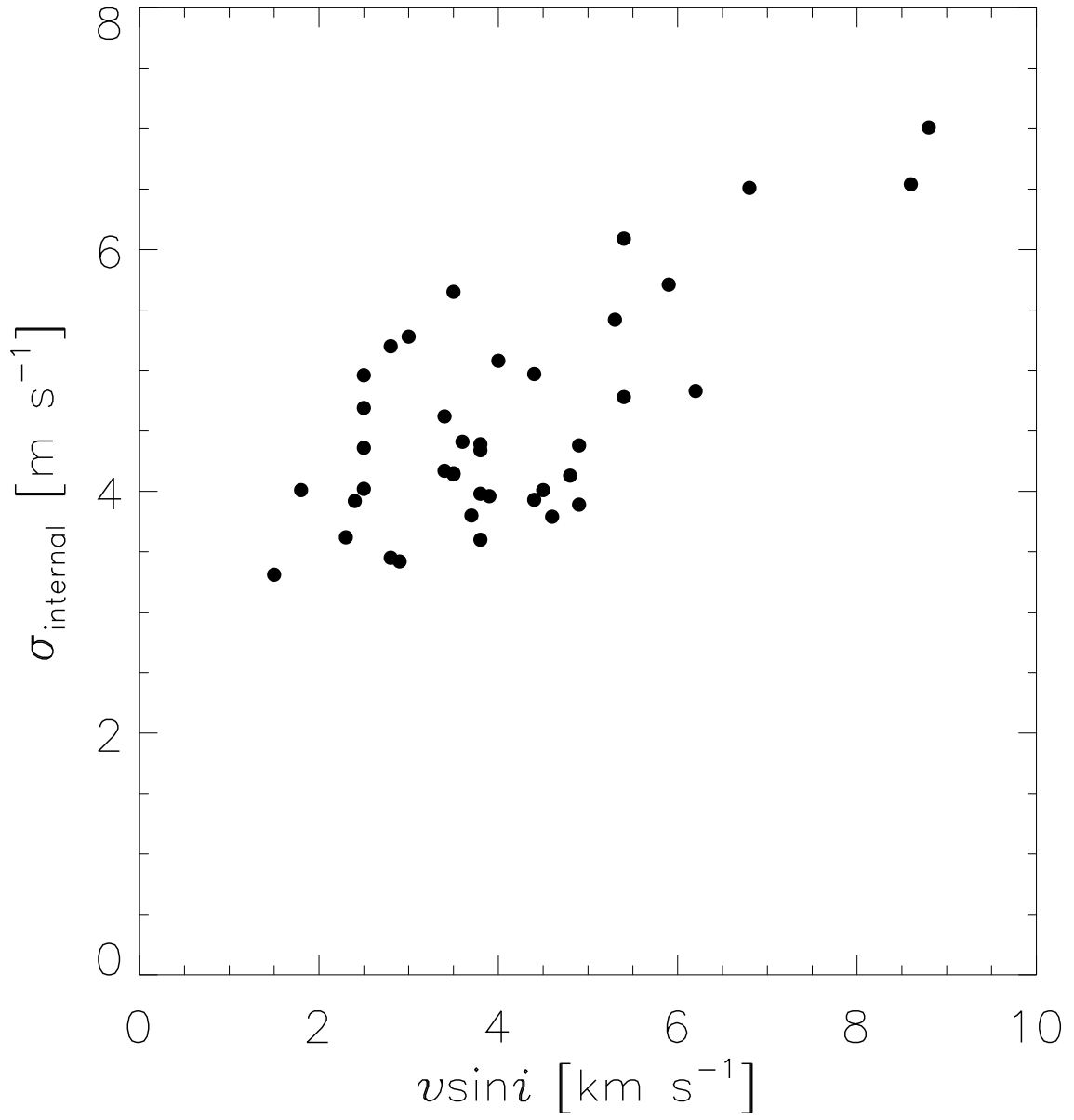


Fig. 4.— Internal errors versus $v \sin i$.

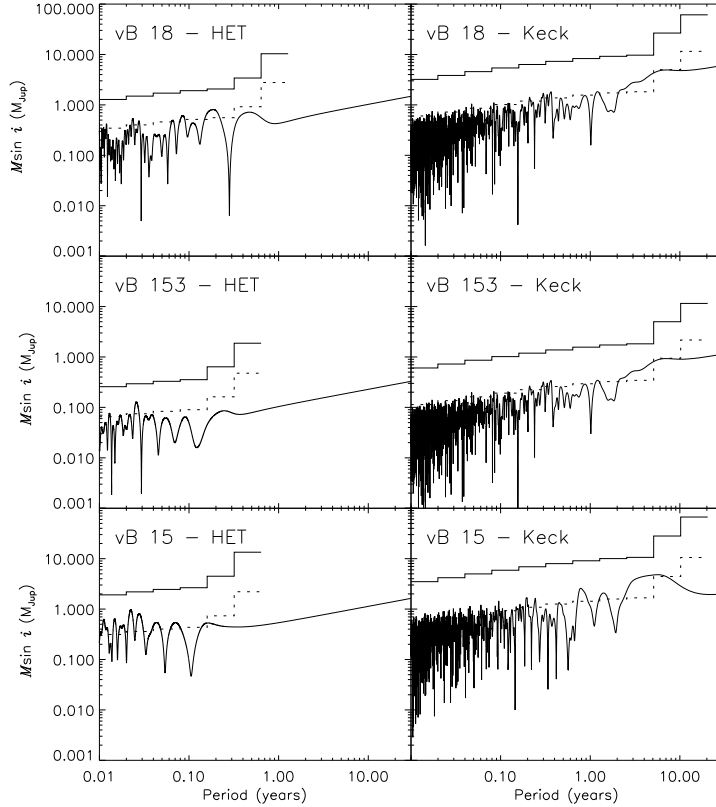


Fig. 5.— The above plots show the limits of our data on the detection of companions. The solid curve represents a power spectrum of the data translated to $M \sin i$ units. The dashed histogram plot, as discussed in the text, is a 99% confidence level for the detection of significant peaks in the data (where a data peak crossing this line would have a 99% confidence of being a true companion). This assumes that the only error for each data point is the internal error of the observations (ranging from about 5-7 m s^{-1}). The solid histogram plot represents a 99% confidence level considering an average error as determined from the rms of v_r caused by stellar activity.

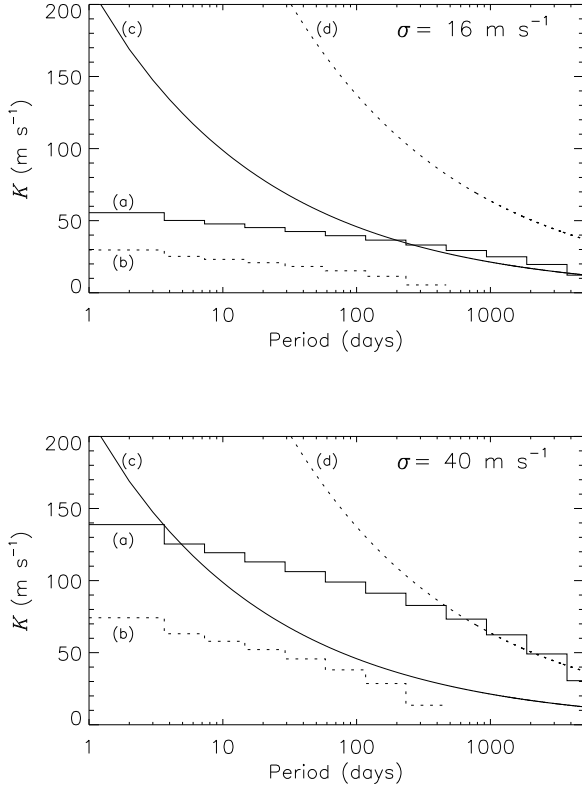


Fig. 6.— Detectability of companions around Hyades-aged stars. The 2 panels represent errors of 16 and 40 m s^{-1} (inclusive of internal errors and radial velocity jitter from stellar activity). Within each panel, the two histograms indicate sampling similar to our Keck data (a) and our HET data (b). For reference, the velocity induced by a $1 M_{Jup}$ planet (c) and a $3 M_{Jup}$ (d) planet around a $1 M_{\odot}$ star (in a circular orbit) for various orbital periods are shown. As in Figure 5, velocity space above the histograms are detectable. So, for example, a $1 M_{Jup}$ planet is just barely detectable if it has a period of only a few days when the errors are the highest in our sample (40 m s^{-1}) but is easily detectable if the same planet has a period of less than 3 months and the error is “average” for the Hyades (16 m s^{-1}).

Table 1. Radial Velocity Observations

Star	JD - 2400000 days	v_r [m s ⁻¹]	σ_{v_r} [m s ⁻¹]
BD+04 810	50792.118	-15.06	5.55
	51076.098	-4.51	2.82
	51441.129	5.76	4.27
	51549.832	10.87	4.48
	51880.897	-5.16	4.05

Note. — The complete version of this table is in the electronic edition of the Journal. The printed edition contains only a sample.

Table 2. Linear Trends and Binaries

Star	slope ($\text{m s}^{-1}/\text{JD}$)	Patience et al.
vA 486	1.7500	N
vB 5	-0.1364	Y
vB 17	-0.0909	Y
vB 52	-0.0333	Y
vB 88	see Table 3	N
vB 184	0.3818	N

Table 3. Orbital Parameters for vB 88

Parameter	Value
$m \sin i$ (M_{\odot})	0.069
Period (days)	2809.2 ± 80.7
V_0 (m s^{-1})	-485.3 ± 5.8
T_0 (JD)	2452100.01 ± 18.9
e	0.5166 ± 0.0123
ω (degrees)	136.45 ± 3.12
K_1 (m s^{-1})	1152.2 ± 15.0

Table 4. v_r Data

Star	$\sigma_{v_r, \text{int}}$ [m s ⁻¹]	σ_{int} [m s ⁻¹]
BD+04 810	10.12	3.92
BD+07 499	15.15	4.52
BD+08 642	12.94	4.73
BD+17 455	11.07	4.01
BD+17 719c	737.05	4.32
BD+19 650	17.56	3.47
HD 18632	10.46	3.42
HD 19902	5.76	3.31
HD 23453	6.82	4.42
HD 26257	7.72	5.71
HD 35768	6.16	4.97
HD 240648	11.85	4.38
HD 242780	8.26	4.13
HD 283869	5.56	3.65
HD 284552	25.63	4.60
HD 284653	14.27	3.62
HD 284930	14.86	4.36
HD 285367	27.47	3.80
HD 285482	13.13	3.73
HD 285590	6.03	3.98
HD 285625	72.92	4.91
HD 285837	16.11	5.92
HD 285849	20.22	6.54
HD 286363	15.98	4.38
HD 286554	13.82	5.18
HD 286734	6.87	3.37
HD 286789	7.45	3.83
HD 286929	6.14	3.99
HIP 15720	5.04	4.66
HIP 16548	17.31	7.11
HIP 17766	9.66	3.71
HIP 19082	22.57	4.98
HIP 22177	9.66	5.71
J 303	3.10	4.79
J 332	12.08	4.75
J 348	7.40	4.54
vA 115	22.81	7.39
vA 146	10.45	5.40
vA 383	5.31	4.64
vA 486 ¹	231.93	39.20
vA 502	10.73	7.19
vA 529	5.91	9.47
vA 637	22.14	6.96
vA 638	8.98	5.84
vA 731	2.63	4.99

Table 4—Continued

Star	$\sigma_{v_r, \text{int}}$ [m s ⁻¹]	σ_{int} [m s ⁻¹]
vB 1	29.87	4.55
vB 2	19.03	4.69
vB 4	13.47	3.45
vB 5 ¹	25.26	3.85
vB 7	16.02	3.60
vB 10	23.62	4.83
vB 12	20.84	4.02
vB 15	40.39	5.12
vB 17 ¹	21.44	4.99
vB 18	31.36	4.78
vB 19	17.11	11.49
vB 21	6.79	3.62
vB 25	8.49	4.36
vB 26	10.33	4.15
vB 27	15.99	3.89
vB 31	27.46	6.54
vB 42	12.45	4.34
vB 46	4.88	5.28
vB 48	21.76	8.92
vB 49	14.15	5.20
vB 52 ¹	15.99	5.81
vB 65	19.91	7.01
vB 66	32.23	6.54
vB 73	21.05	6.51
vB 76	10.14	4.69
vB 79	14.87	4.73
vB 87	15.10	5.18
vB 88 ²	18.44	9.67
vB 92	9.66	4.39
vB 93	53.15	6.09
vB 97	21.05	6.09
vB 99	11.46	4.17
vB 105	15.28	4.96
vB 109	17.09	3.79
vB 118	16.67	5.42
vB 127	12.18	3.98
vB 143	13.92	7.76
vB 153	22.96	4.01
vB 170	17.24	4.09
vB 173	23.99	3.85
vB 174	12.02	3.75
vB 178	12.37	4.14
vB 179	12.31	4.41
vB 180	11.36	3.96
vB 183	8.81	5.65

Table 4—Continued

Star	$\sigma_{v_r, \text{int}}$ [m s ⁻¹]	σ_{int} [m s ⁻¹]
vB 184 ¹	40.52	6.16
vB 187	17.09	3.93
vB 191	2.91	3.93

¹ σ_{v_r} and σ_{int} listed are residuals of the stellar data with linear trends (slopes given in Table 2) removed.

² σ_{v_r} and σ_{int} listed are for residuals of the data with the orbital parameters listed in Table 3 removed.

Table 5. Stars with FAP <10%

Star	P (days)	FAP _{H&B}	FAP _{bootstrap}
vB 7	9.61	0.088	0.045
vB 12	4.04	0.097	0.001
vB 18	17.36	0.040	0.089
vB 19	6.02	0.056	0.006
	4.91	0.089	0.017
vB 87	7.60	0.069	0.088
vB 118	6.15	0.068	0.037
vB 153	4.62	0.010	0.011
vB 170	26.24	0.053	0.014

Table 6. Periods Derived vs. Periods in Literature

Star	$P_{\text{ours,Keck}}$ (d)	P_{HET} (d)	P_{lit} (d)	Reference	P_{pred} (d)	Notes
vB 21	5.49		9	1		
vB 25	4.91		12.6	1		
vB 26	4.6		9.3, 9.4, 9.1	2,1,1	11.22	alias?
vB 31	4.72		5.4	1	4.6	
vB 52	5.64		7.9, 8.0	2,3	5.04	
vB 65	4.65		5.9	1	5.51	
vB 73	12.92		7.4	2,3	5.24	
vB 79	6.13		11.4, 9.7	2,3	12.56	alias?
vB 92	22.53		9	1	9.9	
vB 97	6.45		8.5	2,3	7.46	
vB 173	20.82		14.1	1		
vB 174	10.12		11.9	1		
vB 15	7.43	8.18			6.22	
vB 18	17.36	8.65				alias?
vB 153	4.63	9.42				alias?

¹Radick et al. (1987)

²Lockwood et al. (1984)

³Radick et al. (1995)